Molecular Biology of the Cell
Vol. 14, 1558–1569, April 2003

Role of Microtubules in Fusion of Post-Golgi Vesicles to the Plasma Membrane[V]

Jan Schmoranzer*† and Sanford M. Simon*‡

*Laboratory of Cellular Biophysics, The Rockefeller University, New York, New York 10021; and
†Department of Biology, Chemistry, and Pharmacology, Free University Berlin, 14195 Berlin, Germany

Submitted August 14, 2002; Revised November 6, 2002; Accepted December 4, 2002
Monitoring Editor: Juan Bonifacino

Biosynthetic cargo is transported away from the Golgi in vesicles via microtubules. In the cell periphery the vesicles are believed to engage actin and then dock to fusion sites at the plasma membrane. Using dual-color total internal reflection fluorescence microscopy, we observed that microtubules extended within 100 nm of the plasma membrane and post-Golgi vesicles remained on microtubules up to the plasma membrane, even as fusion to the plasma membrane initiated. Disruption of microtubules eliminated the tubular shapes of the vesicles and altered the fusion events: vesicles required multiple fusions to deliver all of their membrane cargo to the plasma membrane. In contrast, the effects of disrupting actin on fusion behavior were subtle. We conclude that microtubules, rather than actin filaments, are the cytoskeletal elements on which post-Golgi vesicles are transported until they fuse to the plasma membrane.

INTRODUCTION

The cytoskeleton contributes to the transport of biosynthetic cargo from the Golgi to the cell surface. Secretory cargo exits the Golgi in membrane-bounded vesicles whose shapes vary from spheres to elongated tubules. Microtubules have been implicated in exit and transport away from the Golgi in mammalian fibroblasts (Lippincott-Schwartz *et al.*, 2000). Most knowledge of events at the final steps of exocytosis come from studies in neuronal systems where the actin cytoskeleton is thought to be involved in the capture and/or short-range transport of secretory vesicles at the plasma membrane (Lang *et al.*, 2000; Rudolf *et al.*, 2001). Actin-binding proteins, such as synapsin (Huttner *et al.*, 1983), are believed to keep the vesicle in the proximity of the plasma membrane. A number of vesicle-associated proteins, including the RABs (Pfeffer, 1994; Zerial and McBride, 2001), have been implicated in the targeting and docking steps, which are followed by engagement of the cognate vesicular and target soluble *N*-ethylmaleimide-sensitive factor attachment protein receptors and subsequent fusion (Weber *et al.*, 1998). The potential roles of the cytoskeleton in the delivery and fusion of vesicles in the final steps of exocytosis at the plasma membrane are the subject of this study.

Article published online ahead of print. Mol. Biol. Cell 10.1091/mbc.E02–08–0500. Article and publication date are at www.molbiolcell.org/cgi/doi/10.1091/mbc.E02–08–0500.

[V] Online version of this article contains video material for some figures. Online version available at www.molbiolcell.org.

‡ Corresponding author. E-mail address: simon@mail.rockefeller.edu.

Previously, the role of microtubules in post-Golgi traffic has been tested with live cell microscopy and various pharmacological treatments. On depolymerization of microtubules movement of secretory vesicles ceased and secretion of human chromogranin B was slowed (Wacker *et al.*, 1997). Similarly, the saltatory motion of post-Golgi vesicles carrying vesicular stomatitis virus G-green fluorescent protein (VSVG-GFP) stopped after nocodazole treatment; however, the rate of bulk delivery to the plasma membrane was unchanged (Hirschberg *et al.*, 1998). Injection of a function-blocking antibody against kinesin blocked another reporter, p75-GFP, from exiting the Golgi in Madin-Darby canine kidney cells (Kreitzer *et al.*, 2000). Using sequential two-color epifluorescence microscopy, some post-Golgi vesicles loaded with VSVG-GFP colocalized with microtubules in the cytosol of PtK_2 cells (Toomre *et al.*, 1999). These data suggest that microtubules facilitate the transport of biosynthetic cargo away from the Golgi, but also show that microtubules are not absolutely required for secretion.

A number of studies have implicated the cortical actin cytoskeleton in regulated exocytosis. In neurons, synaptic vesicles are embedded, via synapsin, in a meshwork of actin (Humeau *et al.*, 2001). In PC-12 cells, the motility of secretory granules was found to be both limited as well as mediated by the actin cytoskeleton (Lang *et al.*, 2000). The secretory granules are thought to undergo a maturing process while trapped in the actin cortex (Rudolf *et al.*, 2001). Inhibitors of myosin light chain kinase can block mobilization of the reserve pool of secretory vesicles in neurons (Ryan, 1999). Near the cell membrane vesicles are observed embedded in a meshwork of actin. The anchoring may be via synapsin (Huttner *et al.*, 1983; De Camilli *et al.*, 1990), a molecule

whose binding to the vesicle and actin is regulated via phosphorylation (Llinas *et al.*, 1991). However, the role of actin in the final delivery of constitutive post-Golgi cargo has not been resolved.

The final steps in the delivery of post-Golgi vesicles containing GFP-tagged membrane protein to the cell have been examined with total internal reflection-fluorescence microscopy (TIR-FM). These vesicles, upon reaching the cell periphery, moved within a 70-nm plane adjacent to the plasma membrane in a directed manner for distances of microns before fusion (Schmoranzer *et al.*, 2000). The goals of this study were to examine which cytoskeletal components (e.g., microtubules or actin) are responsible for this movement before fusion with the plasma membrane and how fusion changes upon disruption of the relevant cytoskeletal component.

To address these questions we used TIR-FM (Axelrod, 1989) to image this final step of the secretory pathway (Steyer, 1997; Oheim *et al.*, 1998; Schmoranzer *et al.*, 2000; Toomre *et al.*, 2000). In contrast to most assays measuring bulk secretion, we have established a quantitative assay to detect the spatial and temporal distribution of single vesicles fusing with the plasma membrane (Schmoranzer *et al.*, 2000). Using dual-color TIR-FM, we show that post-Golgi vesicles move along the plasma membrane on microtubules up to, and including, the initiation of membrane fusion. This movement is eliminated if microtubules are disrupted and the fusion event is altered with most exocytic fusions failing to completely discharge their cargo. In contrast, we show that depolymerization of the filamentous actin with cytochalasin-D or inhibition of myosin-II and -V ATPases with 2,3-butanedione-monoxime (BDM) slightly shorten the "docking" time before fusion but do not otherwise affect transport and fusion dynamics of constitutive post-Golgi vesicles.

EXPERIMENTAL PROCEDURES

Cell Culture

Normal rat kidney (NRK) fibroblast and MDCK cells were maintained in DMEM (Cellgro; Mediatech, Herndon, VA) supplemented with 10% bovine calf serum and fetal bovine serum, respectively, in a 37°C incubator humidified with 5% CO_2. Cells were plated either onto glass bottom dishes (MatTek, Ashland, MA) or on autoclaved coverslips (Fisher Scientific, Fair Lawn, NJ). For microscopy on stationary NRK fibroblasts, cells were plated at a high enough density such that they reached confluence within 1–2 d. Only cells that were in contact with their neighboring cells were chosen for microscopy.

Nuclear Microinjection

Cells were microinjected with constant pressure into the nucleus with cDNAs encoding the GFP-chimera of 1) the vesicular membrane proteins neurotrophin receptor (p75, 5 μg/ml; Kreitzer *et al.*, 2000), a recycling-deficient mutant of the low-density lipoprotein receptor (LDLRa18, 15 μg/ml); and 2) the microtubule-labeling proteins β-tubulin (10 μg/ml; BD Biosciences Clontech, Palo Alto, CA) and neuronal microtubule-associated protein tau (10 μg/ml). The cDNA was prepared in HKCl microinjection buffer (10 mM HEPES, 140 mM KCl, pH 7.4) and microinjected using back-loaded glass capillaries and a micromanipulator (Narishige, Greenvale, NY). After injection cells were maintained at 37°C in a humidified CO_2 environment for 60 min to allow for expression of injected cDNAs. Newly synthesized protein was accumulated in the Golgi/*trans*-Golgi network (TGN) by incubating cells at 20°C (~3 h) in bicarbonate-free DMEM supplemented with 5% serum and 100 $\mu g/ml^{-1}$ cycloheximide (Sigma-Aldrich, St. Louis, MO). Cells were transferred to recording medium (Hanks' balanced salt solution, supplemented with 20 mM HEPES, 1% serum, 4.5 g/l glucose, 100 $\mu g/ml^{-1}$ cycloheximide). After shifting to the permissive temperature of 32°C for transport out of the Golgi, the arrival of vesicles labeled with p75-GFP or LDLRa18-GFP was monitored by time-lapse total internal reflection-fluorescence microscopy.

All drugs, nocodazole, BDM, and cytochalasin-D were obtained from Sigma-Aldrich.

Image Acquisition

The illumination for TIR-FM was done through the objective as described previously (Schmoranzer *et al.*, 2000). It consists of an inverted epifluorescence microscope (IX-70; Olympus America, Melville, NY) equipped with high numerical aperture lenses (Apo 100× NA 1.65, Apo 60× NA 1.45; Olympus America) and a home-built temperature-controlled enclosure. GFP-tagged proteins were excited with the 488-nm line of an argon laser (Omnichrome, model 543-AP A01; Melles Griot, Carlsbad, CA) reflected off a dichroic mirror (498DCLP). For simultaneous dual-color imaging of cyan fluorescent protein (CFP) and yellow fluorescent protein (YFP), we added two more laser lines and an emission splitter (W-view; Hamamatsu Photonics, Hamamatsu City, Japan). CFP was excited by the 442-nm line of a HeCd laser (Omnichrome, model 4056-S-A02), and YFP was excited by the 514-nm line from an argon laser (Omnichrome, model 543-AP A01). The laser lines were combined by a home-built laser combiner via a dichroic mirror (455DCLP). Both lines (442 and 514 nm) were reflected off a polychroic mirror (442/514pc) The GFP emission was collected through emission band pass filters (HQ525/50 M or HQ550/100 M). The CFP/YFP emissions were collected simultaneously through an emission splitter equipped with dichroic mirrors to split the emission (510DCLP) and emission band pass filters (CFP, HQ480/40 M; YFP, HQ550/50 M). All filters were obtained from Chroma Technologies (Brattleboro, VT).

Images were acquired with a 12-bit cooled charge-coupled device (either Orca I, C4742-95, or ORCA-ER; Hamamatsu Photonics, Bridgewater, NJ) both with a resolution of 1280 × 1024 pixels (pixel size of 6.7 or 6.45 μm^2, respectively). The camera, the NI-IMAQ 1424 image acquisition card (National Instruments, Austin, TX), and a mechanical shutter (Uniblitz; Vincent Associates, Rochester, NY) were controlled by in-house software written in LABVIEW 6.1 by using the IMAQ Vision package (National Instruments). Images were acquired with full spatial resolution at 4–5 frames/s. Images containing a region of interest of the cell were streamed to memory on a PC during acquisition and then saved to hard disk. The number of frames acquired per continuous sequence was limited by the size of the memory (~100–500 kb/image, depending upon the size of the region of interest and the binning mode of the camera). The data was copied onto CD ROM for data storage. The depth of the evanescent filed was typically ~50–60 nm for the Apo 100× NA 1.65 and ~70–120 nm for the Apo 60× NA 1.45 lens (Schmoranzer *et al.*, 2000).

Image Processing and Quantitative Analysis

Processing and analysis of the video sequences was done either with in-house software written in LABVIEW 6.1 using the IMAQ Vision package or with MetaMorph (Universal Imaging, Downingtown, PA).

Temporal Pseudo Dual-Color Processing

Because the microtubule motion is slow compared with the movement of vesicles, we separated the two fluorescent objects tempo-

rally by using a running average algorithm as part of in-house software written in LABVIEW. A running average with a half width of 20 frames was performed on the original sequence. The resulting sequence was called the microtubule channel, because most of the vesicular motions were averaged out and only microtubules remained. Further processing was done in MetaMorph. The microtubule channel was subtracted from the original sequence to yield the vesicle channel, showing only the fast moving objects. The microtubule channel was independently processed with the function "Sharpen," yielding in clear microtubule tracks. Both channels were pseudo color encoded (vesicle, red; microtubule, green), and the maximum signal of each pixel over the entire sequence was projected onto one image, resulting in the overlay of the vesicle tracks on the microtubule tracks.

Quantification of Colocalization of Fusion Sites with Microtubule Tracks in Temporal Pseudo Dual-Color TIR-FM

To confirm colocalization of fusion sites with microtubule tracks, we measured the average intensity of the microtubule channel in small regions (3×3 pixels) around each fusion site ($n = 14$). As a control, we measured the average intensity in the microtubule channel within regions that were devoid of microtubules. The ratio of the microtubule signal at the fusion sites and the background of the microtubule signal was ~50, indicating a clearly positive correlation between vesicular fusion sites and microtubules.

Dual-Color Processing

The original dual-color sequences were acquired through the emission splitter such that the separated channels appear side by side on the camera chip. Processing was done in MetaMorph. Identical regions were cut out of the whole frame to yield separated image sequences. The two channels (CFP and YFP) were aligned within accuracy of one pixel by using a brightfield image taken of the same cell with identical region of interest in dual-color. The YFP channel was corrected for the amount of bleed-through from the CFP channel, which was found to be roughly 50% of the CFP signal. The noise was reduced by performing background subtraction, sharpening and running average. Finally, the separate channels were pseudo color encoded and combined to a RGB sequence.

Quantification of Colocalization of Fusion Site of Tubular Vesicles (p75-YFP) with Microtubule Tracks (tau-CFP) in Simultaneous Dual-Color TIR-FM

To quantify the colocalization of the tubular vesicle (Figure 2c, red) just before fusion with the microtubule tracks (Figure 2c, green), we calculated the average r between both channels for the whole region. To test the quality of correlation the channels were shifted relative to each other in single pixel steps (~110 nm) up to a maximum shift of about ± 1.1 μm in x- and y-direction. The resulting values for the r of all four shift-directions were averaged and plotted (Figure 2e).

Quantification of Colocalization of Tracking Tubular Vesicles (p75-YFP) with Microtubule Tracks (tau-CFP) in Simultaneous Dual-Color TIR-FM

To quantify the colocalization of the moving tubular vesicle (Figure 2c, red) with the microtubule tracks during the last 13 frames before, we compared the average intensity values of the microtubule channel (green) from three different types of regions: 1) regions that do not show microtubules (no MTs), 2) regions that clearly show microtubules (MTs), and 3) regions that overlap with the location of the tubular vesicle during movement until fusion start (tracking tubule). All values are average values from regions manually selected frame by frame such that they add up to similar numbers of pixels. Signal (no MTs) was measured from 30 circular regions (30 pixels each), signal (MTs) was measured from 20 elongated regions of various sizes (~50 pixels each), and the signal (tracking tubule) was measured by manually selected regions around the tubular vesicle for each frame.

RESULTS

Dynamics of Peripheral Microtubules Can Be Visualized within ~100 nm from the Plasma Membrane by using TIR-FM

To visualize single microtubules at the cell surface, we used nuclear microinjection of cDNA encoding either β-tubulin or tau, a neuronal microtubule-associated protein, fused to GFP. In the case of GFP-β-tubulin, we were able to resolve individual labeled microtubules 24 h postinjection in NRK fibroblasts (Figure 1, d–f). At earlier times after injection, the background fluorescence contributed by unincorporated β-tubulin was too high to resolve single microtubules (our unpublished data). In contrast, tau-GFP labeled microtubules within 60 min after microinjection and produced a higher signal-to-background image of the microtubules (Figure 1, a–c). The microtubule network in NRK fibroblasts expressing tau-GFP at 2 h postinjection looked similar to that in cells expressing GFP-β-tubulin at 24 h postinjection. In epifluorescence (A and D), the microtubule-organizing center (MTOC) produce a very bright area, whereas peripheral microtubules are comparably dim. In contrast, in TIR-FM (B and E) of the same cell there were areas of bright and areas of dimmer microtubule tracks, demonstrating that some microtubules were close enough to the plasma membrane to be within the evanescent field, which in this case extended up to ~125 nm from the coverslip. Many microtubules were also visible in TIR-FM if the evanescent field was restricted to <70 nm from the coverslip (using a 100× 1.65 NA objective; see EXPERIMENTAL PROCEDURES; our unpublished data). The variations in fluorescence intensity are due first, to the adhesion pattern of the cell, and second, to the three-dimensional distribution of the microtubules within the cell. The area of the MTOC is dark in the TIR-FM image, showing that the MTOC is outside the evanescent field. The pseudo color overlay (C and F) clearly shows that microtubules are imaged with much higher signal to background in TIR-FM compared with epifluorescence.

In TIR-FM, there are fluorescent tracks that seem to end at points distributed all over the cell surface. From an image at a single time point, it cannot be determined whether these are microtubule ends or intermediate parts of the microtubules that enter and leave the evanescent field. However, in time-lapse TIR-FM (see Videos 1, a and b) we observed distinct microtubules undergoing phases of growth, shortening, and pause, typical of dynamic instability (Mitchison and Kirschner, 1984; Saxton *et al.*, 1984; Schulze and Kirschner, 1986; Sammak and Borisy, 1988). This behavior was observed for microtubules labeled with either tau-GFP or GFP-β-tubulin. Furthermore, we confirmed by immunofluorescence that tau-GFP labels all microtubules (our unpublished data). Thus, because tau-GFP more rapidly labeled the microtubules after microinjection, we used it as a marker for microtubules in our analysis of post-Golgi transport.

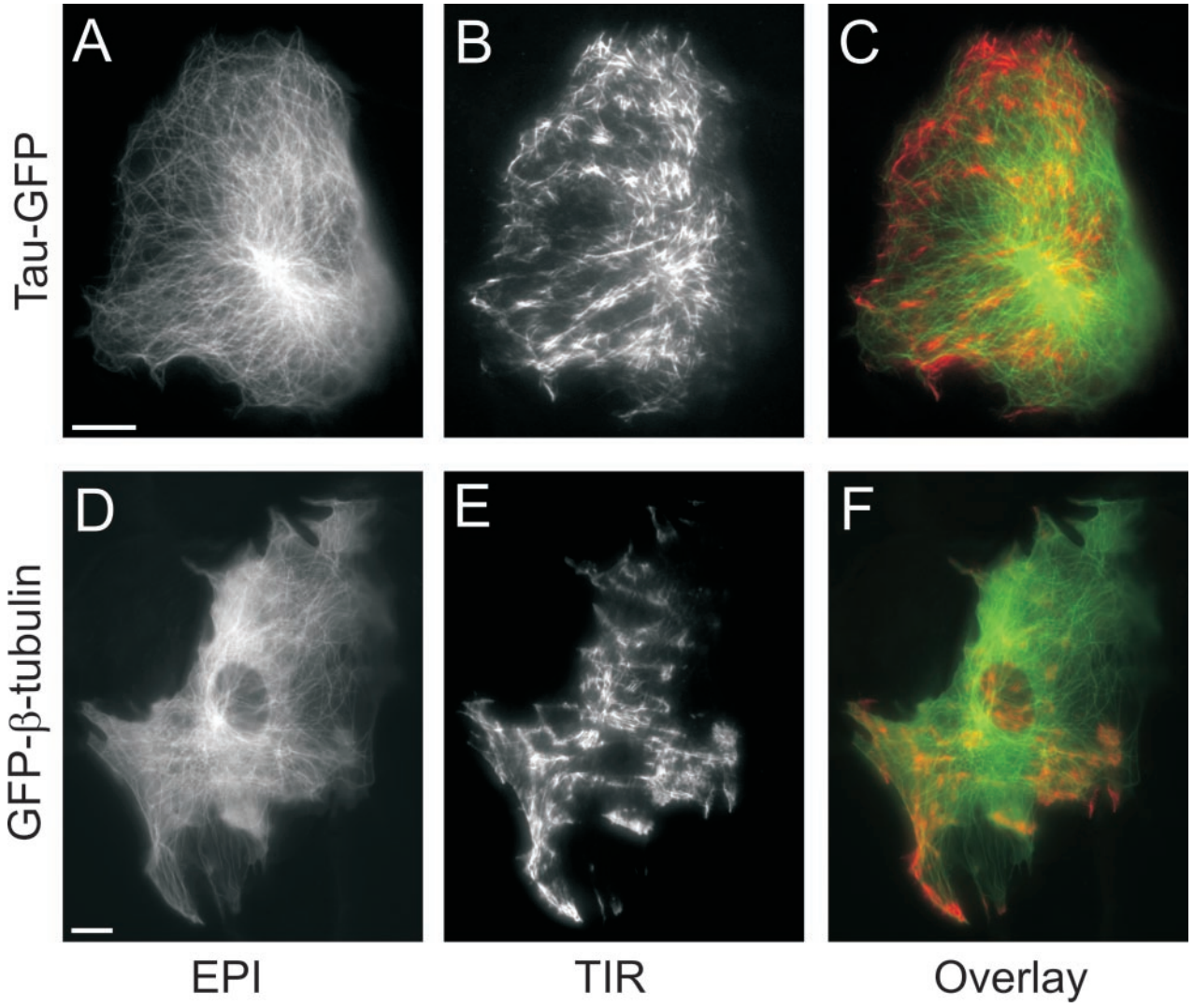

Figure 1. Microtubule cytoskeleton imaged in epi- and TIR fluorescence microscopy. NRK fibroblasts were microinjected with cDNA encoding either tau-GFP at 2 h (A–C) or GFP-β-tubulin at 24 h (D–F) before imaging in epifluorescence (A and D) and TIR-FM (B and E). Pseudo color overlays from the images taken in epifluorescence (green) and TIR-FM (red) are shown (Ca and F). Bars, 10 μm.

Post-Golgi Vesicles Remain on Microtubules until Initiation of Fusion

To characterize the role of microtubules in transport, docking and fusion of post-Golgi vesicles at the plasma membrane, we simultaneously imaged microtubules and membrane proteins as they moved through the biosynthetic pathway. Alternating acquisition of microtubule and membrane cargo images has potential problems of temporal and spatial correlation. Instead, we used two approaches to image the microtubules and the membrane protein cargo simultaneously. The first approach used two different GFP variants, cyan and yellow fluorescent proteins, to differentially label the microtubules and the membrane cargo. Both fluorophores were excited simultaneously and the fluorescence image was split with a dichroic mirror, passed through different emission filters, and then focused side by side on the same cooled charge-coupled device camera (see EXPERIMENTAL PROCEDURES). The second approach took advantage of the very different temporal dynamics of microtubule and vesicle movement. With TIR-FM at high spatial and temporal (>5 frames/s) resolution, it is possible to unambiguously characterize single membrane fusion events (Schmoranzer *et al.*, 2000). In contrast, microtubule dynamics can be resolved by an acquisition speed of $\leq$1 frame/s (Rusan *et al.*, 2001). If it is assumed that all rapid events were due to movement of protein cargo in vesicles and slower events were from movement of microtubules, then the two can be separated by their temporal properties. This latter approach, in which both microtubules and cargo are tagged with GFP, will be referred to as "temporal pseudo dual color." Both approaches gave indistinguishable results.

To image microtubules and post-Golgi vesicles simultaneously, we needed to coexpress reporter proteins that were synthesized and labeled the structures of interest with similar kinetics after microinjection of the cDNAs. As biosynthetic markers, we used a fluorescent protein synthesized as a fusion to the p75 neurotropin receptor (p75-GFP/YFP) or the low-density-lipoprotein receptor (LDLR-GFP), which are both abundantly synthesized within ~1 h after microinjection. Because tau-CFP/GFP was synthesized within 1–2 h after injection without showing significant cytoplasmic background, we chose to coinject the cDNA encoding tau-CFP/GFP, rather than GFP-β-tubulin, together with the cDNA encoding the membrane proteins.

Recently, it was reported that tau expression in mammalian cells affects the attachment of plus-end–directed vesicles to the microtubules, whereas the velocity of movement and the run-length are not altered by expression of tau (Seitz *et al.*, 2002). In our experiments with short-term transient expression of tau-GFP, there were no detectable effects of expression of tau on vesicle movement, docking, or fusion to the plasma membrane as seen in TIR-FM. Thus, the expression level of tau-GFP was low enough in our experiments to allow sufficient attachment of the vesicles to the microtubules at the Golgi and further transport to the periphery.

The overall motion of vesicles labeled with LDLR-GFP/YFP, or p75-GFP/YFP observed in TIR-FM in NRK cells was very similar to the motion we previously observed with VSVG-GFP–labeled vesicles. As previously characterized, their motion at the plasma membrane could be classified, as defined below, into a transport phase, a stationary phase, and a fusion phase (Schmoranzer *et al.*, 2000).

Transport Phase: Movement of Vesicles along Microtubules on the Cell Surface

Vesicles containing p75-GFP moved in curvilinear tracks when in close proximity (<125 nm) to the plasma membrane. In dual-color TIR-FM these tracks were always spatially coincident with the tau-GFP–labeled microtubules (Figure 2b and Video 2a). The overall movement of p75-GFP–containing vesicles along tau-GFP–labeled microtubule tracks was indistinguishable from their motion in cells that were not injected with tau-GFP. The transport of membrane cargo along microtubules occurred in the typical saltatory manner, alternating between fast and slow movements (video 2a) and the vesicles frequently switched between different microtubule tracks. Some vesicles reached the edge of the cell, whereas others stopped even though they had not reach the end of a microtubule.

Stationary Phase: Docking of Vesicles along Microtubule Tracks

The transport phase was followed by a stationary phase, during which the vesicles did not leave an area with a radius of ~100 nm (see EXPERIMENTAL PROCEDURES). The duration of this phase between cessation of directed transport and the start of the fusion, which we will refer to as the docking phase, turned out to have a broad distribution with a mean of 15.1 ± 12.4 s (n = 57) in untreated cells (Figure 5, untreated cells).

Fusion Phase: Fusion of Vesicles along Microtubule Tracks

Many vesicles were observed to brighten followed by a rapid lateral spread and dilution of the GFP fluorescence. The following criteria were used to determine whether such a vesicle had either 1) fused to the plasma membrane, 2) photolysed, or 3) moved away from the membrane (Schmoranzer *et al.*, 2000). A vesicle that fuses delivers its membrane protein cargo to the plasma membrane. This can be detected by two distinguishing characteristics. The first characteristic is the total GFP fluorescence intensity of the vesicle. As the vesicle gets closer and then fuses to the membrane, the total intensity increases (because the fluorophores are moving deeper into the evanescent field). If all the fluorophores are delivered to the membrane, no fluorescence is lost and the total intensity rises to a new plateau. The second characteristic is the Gaussian width of the fluorescence. After fusion of the vesicle the membrane proteins diffuse laterally into the plasma membrane. The area (width^2) increases linearly with time, and the slope is the diffusion constant of the marker protein in the plasma membrane. In contrast, a vesicle that lysed would not deliver its cargo to the plasma membrane. Rather, the cargo would diffuse into the cytoplasm. As a result, there would be a brief increase in total intensity as it moved closer to the membrane followed by a rapid decrease rather than a plateau in the total fluorescence. Furthermore, the width^2 would increase significantly more rapidly because the diffusion of proteins in the cytoplasm is much faster than diffusion in a membrane. Thus, in all presumed fusion events two critical parameters were quantified: the total integrated intensity and the width^2.

Using these criteria, we mapped where vesicles containing p75-GFP fused with the plasma membrane of NRK fibroblasts (Figure 2, a and b). Within our optical lateral resolution (~250 nm) and temporal resolution (~200 ms) the center of the fusions (white crosses in the still image and white arrows in the video) always colocalized with the microtubule tracks as observed in temporal pseudo dual color TIR-FM (see EXPERIMENTAL PROCEDURES). The microtubule fluorescence signal at fusion sites (n = 20) was ~50 times higher than the background (see EXPERIMENTAL PROCEDURES). This is consistent with colocalization of microtubules and fusion sites and with the possibility that secretory vesicles do not detach from microtubules before they reach their site of fusion.

The experiments were repeated with simultaneous dual-color TIR-FM in cells expressing tau-CFP and p75-YFP. This approach has the advantage that we do not have to make assumptions about the temporal behavior of the proteins being imaged. However, it required polychroic mirrors for excitation and additional dichroic mirrors and narrow bandpass filters to split the emission. Thus, the fluorescent signal was decreased relative to the previous approach. To still be able to monitor fusion in simultaneous dual color, we used MDCK cells expressing p75-YFP, in which many post-Golgi vesicles are highly fluorescent tubules that can be up to many micrometers in length (Hirschberg *et al.*, 1998; Kreitzer *et al.*, 2000). All movement of the vesicles was coincident with the microtubules and all fusions occurred along microtubule tracks. One tubular post-Golgi vesicle loaded with p75-YFP is shown tracking along the microtubules (Figure 2c and Video 2b). It bends while switching tracks, and

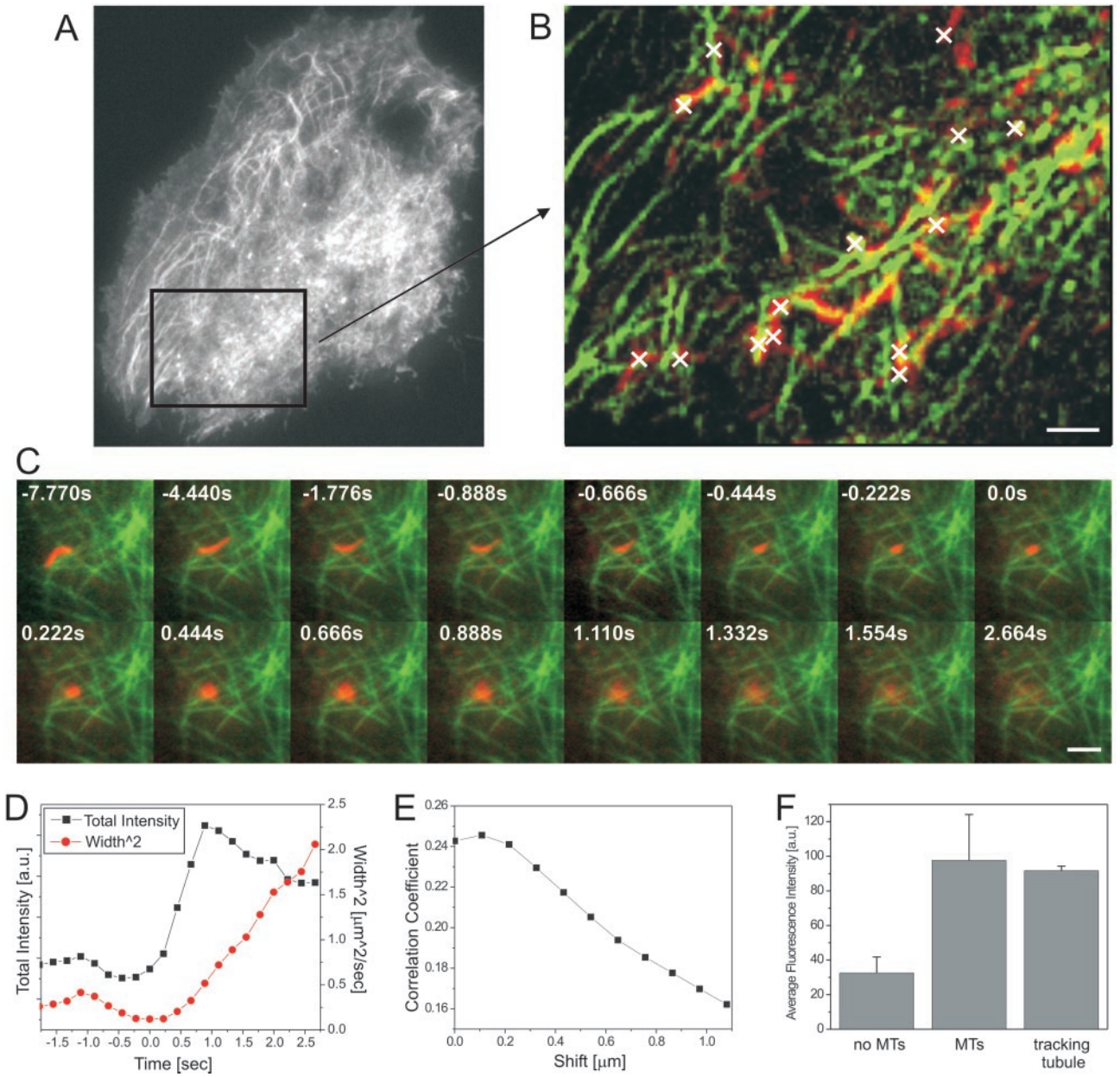

Figure 2. Transport, docking, and fusion of vesicles along the microtubule cytoskeleton imaged in dual-color TIR-FM. (A and B) The nucleus of a NRK fibroblast was microinjected with cDNA encoding p75-GFP and tau-GFP and imaged in TIR-FM with a temporal resolution of ~5 frames/s. The sequence was processed according the protocol for temporal pseudo color TIR-FM to separate the fast moving vesicles from the slow motion of the microtubule cytoskeleton (see EXPERIMENTAL PROCEDURES). A region of the whole cell A is shown in B. To reveal the colocalization of the vesicle tracks (red) with the microtubule tracks (green), the maxima of each pixel of the separated sequences were projected onto a single image (B). The fusion sites are marked as white crosses. (C) A MDCK cell was microinjected with cDNA encoding p75-YFP and tau-CFP and imaged in simultaneous dual color TIR-FM with a temporal resolution of ~5 frames/s. The sequence was processed according to the protocol described below, including bleed-through correction and contrast enhancement (see EXPERIMENTAL PROCEDURES). A tubular vesicle containing p75-YFP is shown (red) to track, collapse, and fuse along the microtubule tracks (green). The time is indicated relative to the start of fusion. (D) Measured values for the total and the width^2 of the intensity of the fusing tubular vesicle (C). (E) To quantify the colocalization of the tubular vesicle (C; red) just before fusion with the microtubule tracks (C; green), we calculated the average r between both channels for the whole region. To test the quality of correlation the channels were shifted relative to each other about ± 1.1 μm in x- and y-direction in 108-nm steps, respectively. The resulting values for the r were averaged (E). Bars, 2 μm. (F) To quantify the colocalization of the tubular vesicle (C; red) with the microtubule track during the movement just before the fusion (13 frames before fusion start), we compared the average intensity values of the microtubule channel (green) from three different types of regions: 1) regions that do not show MTs (no MTs), 2) regions that clearly show MTs (MTs), and 3) regions that overlap with the location of the tubular vesicle during movement until fusion start (tracking tubule). The average values and their SD are displayed in the graph.

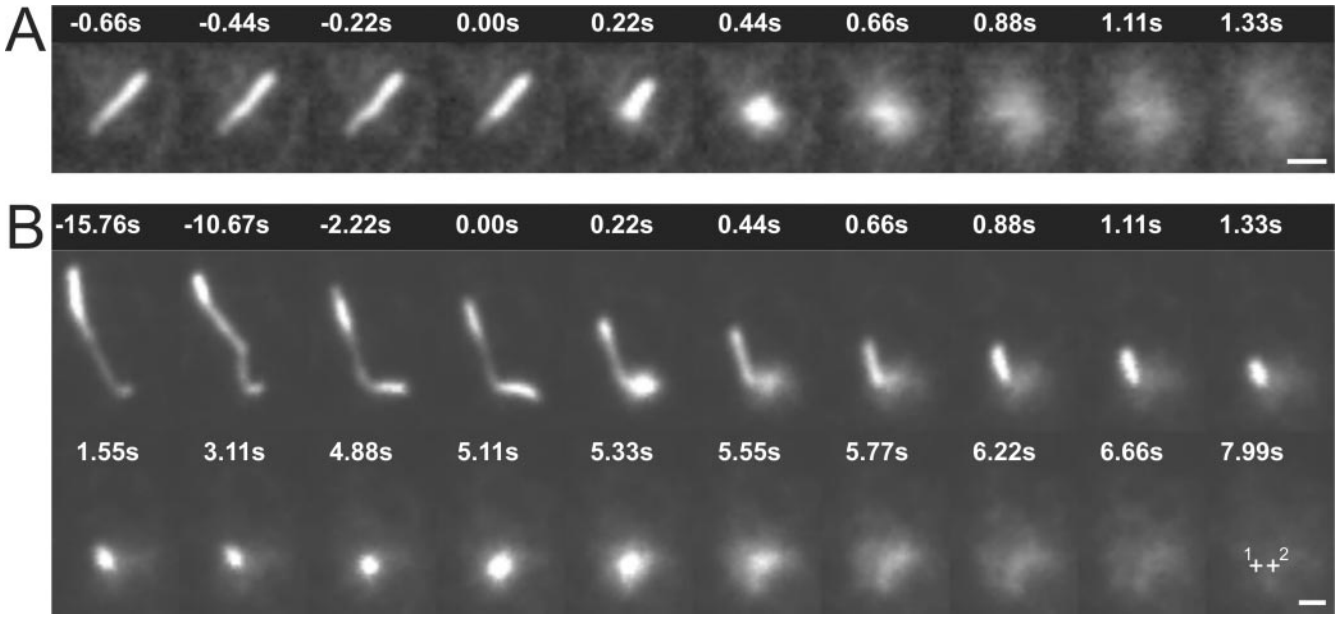

Figure 3. Collapse and fusion of tubular vesicles. Sparsely plated MDCK cells were microinjected with cDNA encoding p75-GFP and imaged in TIR-FM after release of the Golgi block (see EXPERIMENTAL PROCEDURES). Tubular vesicles loaded with p75-GFP were seen to collapse and fuse both in a single step (A) and in two steps (B). For both vesicles, the time is indicated relative to the fusion start. For the two-step fusion (B), the second fusion starts at 4.88 s. The center of each sequential fusion are labeled with crosses (1 and 2) in the last frame (time = 7.99 s), indicating that vesicle was displaced by ~0.5 μm just before the start of the second fusion. Bars, 1 μm.

moves back a small distance, until it collapses and fuses along the microtubule track. The quantification clearly shows the simultaneous rise of total and width^2 of the fluorescence intensity characteristic for all fusion events (Figure 2d). The dip in the width^2 just before fusion start indicates the collapse of the membrane tubule. To test for colocalization of the fusing vesicle with the microtubule track, we performed a spatial cross-correlation analysis between the p75-YFP and the tau-CFP (see EXPERIMENTAL PROCEDURES) for the time point just before fusion. The radially averaged r clearly shows a peak at zero-shift between the two channels within ±100 nm (Figure 2e; see EXPERIMENTAL PROCEDURES). Furthermore, we checked for colocalization of the tubule with the microtubules during the last 13 frames of its movement before fusion (Figure 2f; see EXPERIMENTAL PROCEDURES). The average fluorescent signal in the microtubule channel at the location of the tracking tubule is almost indistinguishable from the average signal of regions containing microtubules (MTs). Furthermore, it is ~2.8-fold higher than the signal of the microtubule channel from regions not containing microtubules (no MTs). This indicates that the tubule follows the MT tracks until it fuses. Together, these data confirm the observation obtained by temporal pseudo dual-color TIR-FM that vesicles fuse along microtubule tracks.

Fusion of Vesicles to Plasma Membrane

Post-Golgi vesicles are seen in a distribution of shapes from spheres to elongated tubules (Hirschberg *et al.*, 1998; Toomre *et al.*, 1999; Kreitzer *et al.*, 2000; Schmoranzer *et al.*, 2000). The fraction of vesicles that were tubular or spherical varied greatly between cell types and constructs. Previously, using VSVG-GFP as membrane cargo expressed in COS-1 cells, we observed that tubular vesicles underwent a rapid shortening, or "collapse," of the tubular morphology shortly before, or at the onset of dispersal of the cargo into the plasma membrane (Schmoranzer *et al.*, 2000). This "collapse and fusion" of tubular vesicles was subsequently observed in various cell types (NRK fibroblasts and subconfluent MDCK cells) by using different membrane cargo (LDLR-GFP and p75-GFP). It was always seen when the tubular morphology was clearly resolved (when the tubule was oriented parallel to the coverslip in the evanescent field). An example demonstrating fusion of an elongated vesicle is shown in Figure 3a (also see Video 3a).

Single and Multiple Fusions from Individual Vesicles

In ~87% of all analyzed fusion events (n = 534, 8 cells) all the membrane cargo was delivered into the plasma membrane in a single step (Figure 3a and Video 3a). This process we will call "complete fusion." The remaining ~13% of fusions showed "partial release." Only a part of the cargo was delivered into the plasma membrane during the fusion event, leaving a significant amount of fluorescence signal behind. These partial release fusions were seen for both spherical and tubular vesicles in all cell types examined. Some of these were multiple fusions and release of the same vesicle at the same spot, and in other cases the same vesicle fused at multiple discrete locations. This latter example is perhaps closest to the proposed model of "kiss and run" in

Table 1. Quantitative characterisation of exocytic fusions in untreated and nocodazole treated NRK cells

	No treatment	Nocodazole
Rate of exocytosis	8 fusions/min (181 fusions, 4 cells)	4 fusions/min (185 fusions, 4 cells)
Fusions that result in complete release	86% of all fusions (n = 181, 4 cells)	45% of all fusions (n = 185, 4 cells)
Fluorescence release/vesicle	2500 ± 1700 fluorescent units (n = 33)	3900 ± 2300 fluorescent units (n = 30)
Docking time	15.1 ± 12.4 s (n = 57)	No movement
Percentage of tubular vesicles	29.9% (*n* = 147, 5 cells)	4.2% (*n* = 226, 5 cells)

regulated in exocytosis (Fesce and Meldolesi, 1999). This type of partial fusion was most clearly resolved as multiple fusions from a single tubular vesicle. An example of one 6-μm-long tubule is shown from an MDCK cell (Figure 3b and Video 3b). At t = 0 there was an initial fusion delivering ~45% of the total membrane cargo. This fusion was coincident with an abrupt shortening of the rest of the tubule. During the shortening event the tubule moved toward the fusion site with a maximum speed of ~5 μm/s. This value is at least twofold faster than reported maximum speeds for kinesin mediated vesicle movements on microtubules (2.5 μm/s) (Trinczek *et al.*, 1999). This collapse of the vesicle along the microtubule is similar to what was shown in the simultaneous dual-color imaging (Figure 2c). However, in Figure 3b the vesicle does not collapse fully into the fusion center. The first fusion and shortening was followed by a 3- to 4-s-long stationary phase. Then, the tubule fused a second time to a spot shifted by ~0.5 μm relative to the first fusion site (Figure 3b, crosses). During the second fusion event all remaining cargo diffused in the plasma membrane.

Nocodazole and Vesicle Fusion

The role of microtubules in exocytosis was examined by imaging the fusion of post-Golgi vesicles at the plasma membrane using TIR-FM in untreated and in nocodazole-treated stationary NRK cells. NRK cells were grown to confluence for 2 d such that each cell was in contact with neighboring cells. We expressed the membrane protein LDLR-GFP via nuclear microinjection and accumulated newly synthesized protein in the Golgi/TGN by incubating the cells at 20°C. Vesicles were observed to fuse to the plasma membrane within 10 min after release of the Golgi block. This continued with an average rate of ~8 fusions/min (181 fusions in 4 cells; Table 1) until the Golgi was completely empty, which sometimes took >60 min.

When NRK cells were treated with 10 μM nocodazole during the last hour of the Golgi block, microtubules were largely, but not completely, depolymerized, resulting in a partially dispersed Golgi (our unpublished data). Two major changes occurred after nocodazole treatment. First, the vesicles showed very little directed transport. Second, elongated tubular vesicles were no longer seen in any cell type or with any cargo molecules. This strongly suggests that tubular morphology is due to the attachment to microtubules and the rapid collapse during fusion was a consequence of detachment from the microtubules. Despite these changes, fusion events were still observed, albeit at a reduced rate (~4 fusions/min, 185 fusions; Table 1).

When 10 μM nocodazole was added 30 min after microinjection and kept in the medium during the 3-h Golgi block, the microtubule array completely disassembled and the Golgi was fully dispersed into small fragments throughout the cytoplasm (our unpublished data). Under these conditions fusion was observed close to the Golgi elements (our unpublished data) and the rate of fusion (~4 fusions/min, 68 fusions) was similar to that of the shorter nocodazole treatments. Again, we did not observe directional transport of any vesicles by TIR-FM.

Furthermore, the fusion events in nocodazole-treated cells differed from the events in untreated cells. There was a significant increase in the frequency with which vesicles had to fuse multiple times to discharge their cargo. In untreated stationary cells there was only a partial delivery of the vesicular membrane proteins to the plasma membrane in ~14% of exocytic fusions (n = 181 in 4 cells; Table 1). This was independent of whether the vesicle was spherical or tubular.

In nocodazole-treated cells most of the labeled secretory cargo was close to the cell center in very large and static fluorescent spots. Some of these compartments were visible in TIR-FM and they fused to the plasma membrane. However, most only delivered part of their membrane cargo and underwent frequent fusions at the same spot on the plasma membrane (Figure 4). Even the repeated fusions did not always result in the complete emptying of the compartment. These fusions were observed, as before, as an increase total fluorescence, accompanied by a spread of fluorescence. However, a bright spot was left behind. This spot alternated between static phases and repeated discharge of cargo into the plasma membrane in subsequent fusion events. Nocodazole treatment also quantitatively changed the amount of cargo, which was delivered during each fusion. In untreated cells the average amount of fluorescent membrane cargo delivered was ~2500 ± 1700 fluorescent units (n = 33; Table 1), whereas in nocodazole-treated cells the distribution broadened and the average value increased to ~3900 ± 2300 fluorescent units (n = 30; Table 1) (unpaired Student's *t* test, $p < 0.01$). These repeated fusions may originate from the dispersed Golgi ministacks, which are in proximity to the plasma membrane. For the short-term (1-h) incubation in nocodazole ~55% of all fusions (n = 185; Table 1) were partial (including repeated fusions) and for the longer term (3.5-h) incubation ~49% of all fusions (n = 68) were partial (including repeated fusions). This is more than a threefold increase compared with the untreated cells.

Actin Cytoskeleton and Docking Time of Vesicles

Two pharmacological treatments were used to test whether the actin cytoskeleton plays a role in constitutive exocytosis. First, we depolymerized the actin cytoskeleton with the

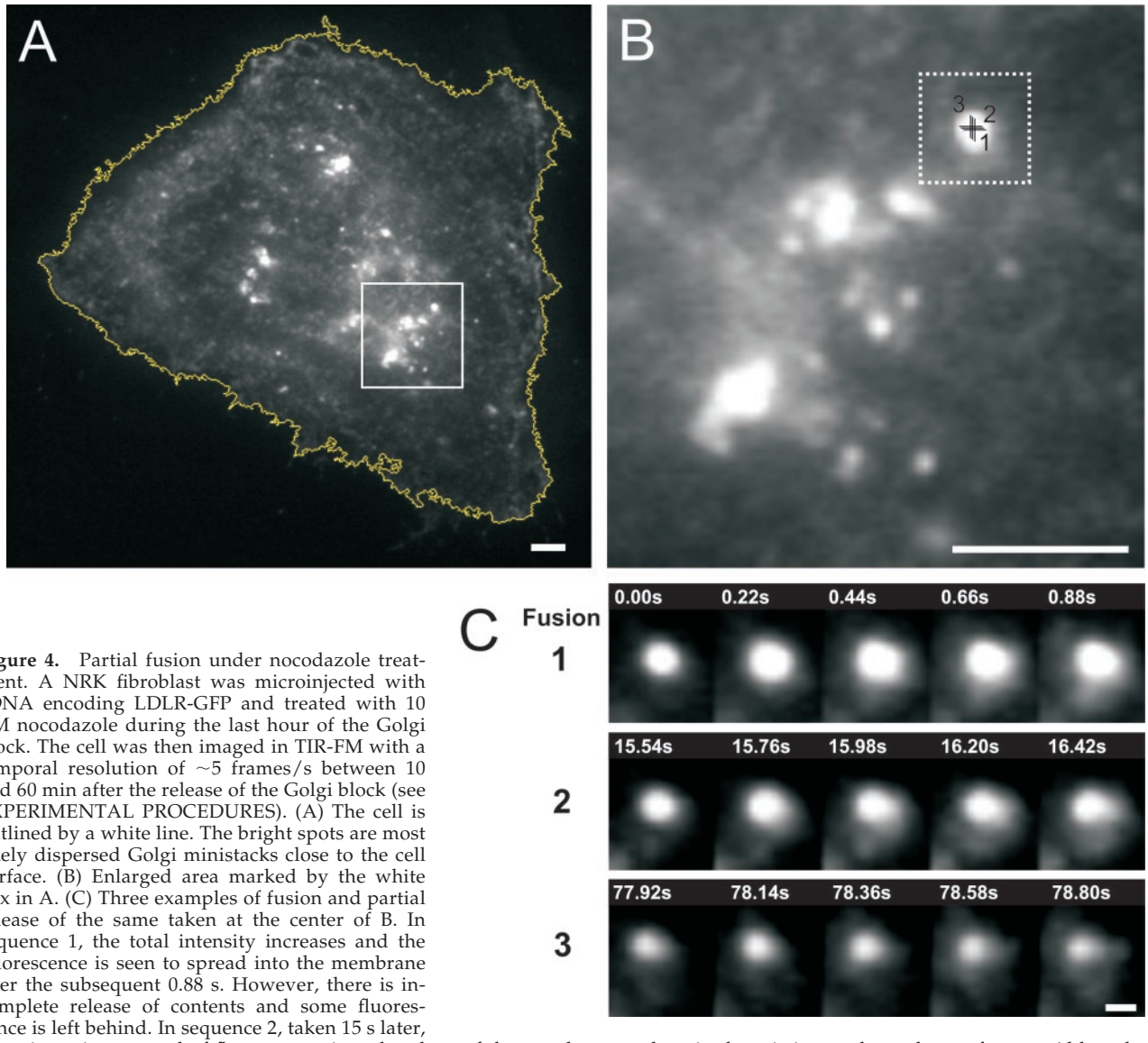

Figure 4. Partial fusion under nocodazole treatment. A NRK fibroblast was microinjected with cDNA encoding LDLR-GFP and treated with 10 μM nocodazole during the last hour of the Golgi block. The cell was then imaged in TIR-FM with a temporal resolution of ~5 frames/s between 10 and 60 min after the release of the Golgi block (see EXPERIMENTAL PROCEDURES). (A) The cell is outlined by a white line. The bright spots are most likely dispersed Golgi ministacks close to the cell surface. (B) Enlarged area marked by the white box in A. (C) Three examples of fusion and partial release of the same taken at the center of B. In sequence 1, the total intensity increases and the fluorescence is seen to spread into the membrane over the subsequent 0.88 s. However, there is incomplete release of contents and some fluorescence is left behind. In sequence 2, taken 15 s later, there is again a spread of fluorescence into the plane of the membrane and again there is incomplete release of cargo. Although this time there is considerably less fluorescence left behind. In sequence 3, taken 78 s later there is another of spread of the fluorescence. Bars, 3 μm (A and B) and 0.5 μm (C).

drug cytochalasin-D. Second, we used the drug BDM, which has been used to inhibit the myosin-II and -V light chain kinases and lead to inhibition of postmitotic cell spreading in fibroblasts (Cramer and Mitchison, 1995). Treatment with either 10 mM BDM or 1 μM cytochalasin-D had no detectable qualitative effect on the transport and fusion of vesicles carrying LDLR-GFP in NRK cells. In addition, the distribution of fusion sites was unaffected by BDM treatment (our unpublished data).

The actin cortex is thought to play several roles in regulated exocytosis, including the capture and transport of secretory granules (Lang *et al.*, 2000; Rudolf *et al.*, 2001) and synaptic vesicles close to the plasma membrane (Ryan, 1999). If actin is involved in constitutive exocytosis, we assumed that the time between the cessation of directed transport and the start of fusion (which we call the docking time) would be sensitive to changes in properties of the actin cytoskeleton during this phase. Thus, we measured the docking time of post-Golgi vesicles in cells. In control cells the docking time of vesicles had a broad distribution with a mean of 15.1 $\pm$ 12.4 s (n = 57) (Figure 5). The docking time was decreased by one-third to 10.6 $\pm$ 6.7 s, n = 61 (unpaired Student's *t* test, $p < 0.05$) when 10 mM BDM was present to the media. Treatment with cytochalasin-D (1 μM for at least 10 min) also decreased the docking time (9.5 $\pm$ 9.5 s, n = 52; unpaired Student's *t* test, $p < 0.01$). Fusion could be monitored for up to 60 min in the presence of cytochalasin-D application without observing major retractions of the cell body under TIR-FM.

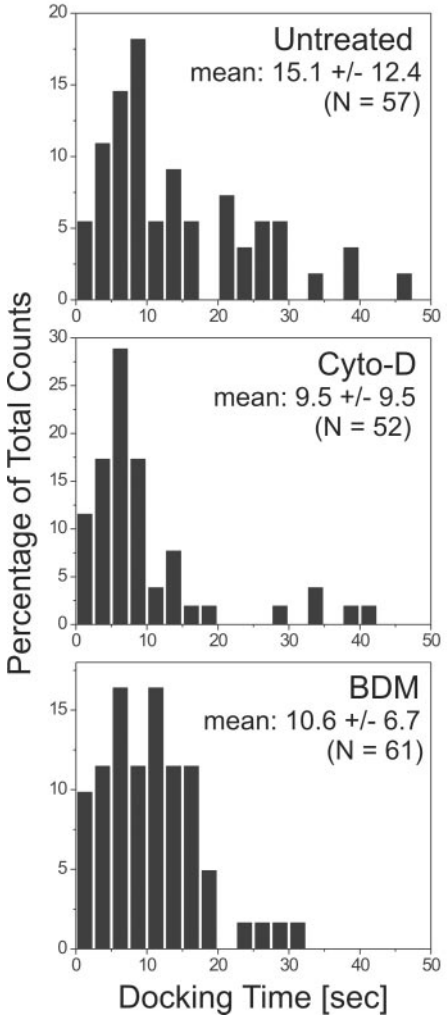

Figure 5. Histogram of docking times measured for vesicles. NRK fibroblast were microinjected with cDNA encoding LDLR-GFP and imaged in TIR-FM as described above. The docking times (see text for definition) of vesicles ($n > 50$) were measured for untreated, cytochalasin-D–treated, and BDM-treated cells. The mean value of the docking times their SD, the p values for comparison of control and drug treatment and the sample size is indicated. Drugs were added for at least 5 min before acquisition. The counts are normalized to the total counts.

Depolymerization of the actin cortex with cytochalasin-D can result in changes of the cell morphology and adhesion pattern, which poses potential problems for TIR-FM. In these experiments, treatment with 1 μM cytochalasin-D for 10 min was sufficient to depolymerize many of the stress fibers as observed by immunofluorescence (our unpublished data). However, because the cells were still attached to the coverslips, we assume that at least some of the actin filaments and structures were still intact. It is possible that after treatment with cytochalasin-D, the residual filamentous actin was sufficient for supporting constitutive exocytosis.

DISCUSSION

Previously, we reported that post-Golgi vesicles carrying secretory membrane cargo move within a 70-nm plane along the cell surface in a directed manner shortly before they fuse with the plasma membrane (Schmoranzer *et al.*, 2000). This raises the question of which cytoskeletal element is responsible for the transport just before fusion. Herein, we show that microtubules are actively moving adjacent to the membrane in living NRK cells (Figure 1), TC-7 cells, and subconfluent MDCK cells (our unpublished data). This demonstrates that at least in some tissue culture cell lines, the actin cortex at the contact surface is either extremely thin (<100 nm) or can be penetrated by microtubules. Vesicles, in turn, move along the microtubules until they exocytose.

Our results demonstrate several important roles of microtubules in the exocytosis of vesicles. First, microtubules determine the morphology of the vesicles. Neither tubular vesicles, nor their collapse and fusion ever occurred in cells devoid of microtubules. This suggests that the tubular shape observed in some vesicles is a consequence of attachment at multiple points to the microtubules.

A second role for microtubules is to transport vesicles (independent of their morphology) not just to the periphery but to their site of fusion at the plasma membrane. This conclusion is based on a few observations. In all cases fusion sites could not be spatially resolved from the microtubules. Thus, if vesicles leave the microtubules before fusion, then all the vesicles we have imaged must fuse within ~200 ms (the rate at which we acquired images). Furthermore, vesicles were only observed as tubules in the presence of microtubules and they maintained their morphology and thus were still attached to the microtubules until the initiation of fusion. Finally, upon fusion, tubules were observed to collapse into the point of fusion. This collapse followed the microtubules (Figures 2C and 3B). These results indicate vesicles are on microtubules when they start to fuse. Therefore, it is not necessary to invoke additional machinery to keep the vesicles docked in the vicinity of the plasma membrane before fusion.

Collapse of the elongated tubule during fusion may coincide with release of microtubule attachments. The speed of tubule collapse was significantly faster than any reported kinesin-dependent transport, suggesting that a release of membrane tension rather than microtubule motors plays a role in this process. It has been proposed that cell surface area may be regulated by the local addition of membrane during exocytosis to compensate for high plasma membrane tension (Morris and Homann, 2001). High tension in the plasma membrane relative to the tubule membrane could explain the acceleration of the tubule collapse. It could explain why large tubular vesicles seem to be actively pulled toward their site of fusion. The equilibration of tension gradients, for the small spherical vesicles may also occur, but extremely quickly, potentially too fast to be resolved by standard imaging techniques.

A third, perhaps more speculative, role for the microtubules is in affecting the dynamics of the fusion event. The frequency of partial fusions, a rare event in control cells (~13%), dramatically increased in nocodazole-treated cells (~54%). Vesicles frequently move along within 100 nm of the plasma membrane surface before docking and fusing (Schmoranzer *et al.*, 2000). This movement, which is micro-

tubule-dependent (Figure 2, A–C) may be facilitating the coupling of many copies of the fusion machinery between the vesicle and the plasma membrane. In the absence of this microtubule-dependent movement the fusions may be more likely to reverse and disengage before the complete discharge of cargo.

Our observations exclude some roles for the microtubules. The microtubule on which a vesicle travels does not uniquely determine where the vesicle will fuse. Adjacent to the plasma membrane the tubular vesicles frequently move along sharp bends (Videos 2C and 3B), which suggests that each vesicle can be attached to multiple crossing microtubules at the same time. This indicates that the targeting of these vesicles cannot be solely attributed to a "master" sorting machinery at the TGN that loads cargo onto specific microtubules for a particular target site at the plasma membrane. This is consistent with previous observations demonstrating that on the interior of the cell vesicles can switch between microtubules (Hirschberg *et al.*, 1998; Toomre *et al.*, 1999). Furthermore, we observed that vesicles can fuse at sites where microtubules are continuous, in other words, the vesicles do not have to reach the end of the microtubules in order to fuse. Thus, the fusion sites are not determined by the ends of microtubules.

It has been suggested that in the middle of the cell vesicles moving on microtubules have a distinct "head" and "tail" domains (Stephens and Pepperkok, 2001). Interestingly, in our observations of collapsing and fusing vesicular tubules, the center of fusion is not restricted to the end of a tubule. This suggests that formation of a fusion pore can be achieved anywhere along the vesicle wherever it engages the fusion machinery at the plasma membrane. This is consistent with the observation from recent correlative light-electron microscopy studies showing that post-Golgi vesicles are highly amorphous structures, rather than simple cylindrical tubes, as seen in light microscopy (Polishchuk *et al.*, 2000).

Our results leave open the question about the mechanism of transport and fusion of membrane cargo in the absence of microtubules. Delivery could be mediated either by direct fusion of intracellular organelles to the plasma membrane or by tubular extensions off the organelles which fuse directly to the plasma membrane. Alternatively, transport intermediates could bud off and fuse to the closest part of the plasma membrane. Either way, our results show that intact microtubules are is responsible for the site-directed fusion of vesicles.

The necessary and sufficient components of the fusion machinery in vivo are still not fully known. Many results suggest the existence of cognate SNARE pairs that dictate the specificity of fusion between different membrane compartments (McNew *et al.*, 2000). The observation that sites of fusion are dramatically redistributed upon disrupting microtubules suggests either that localization of the fusion machinery is microtubule dependent or that the fusion machinery is normally present all over the cell and localized fusion is a consequence of localized delivery.

Although the actin cortex has been suggested to play several roles in regulated exocytosis, our results do not indicate a significant role for actin in constitutive exocytosis. Neither inhibition of myosin ATPases with BDM, nor depolymerization of filamentous actin with cytochalasin-D, had a gross effect on transport, docking or fusion of vesicles. However, we did find that cytochalasin-D or BDM treatment resulted in a one-third decrease in the average time a vesicle was docked adjacent to the membrane before fusion. This suggests that clearing away actin facilitates fusion and that in flat tissue culture cells like NRK fibroblasts, transport along filamentous actin is not required for constitutive exocytosis. This excludes the necessity of a "dual-transport" mechanism in which single vesicles carry motors enabling transport on both, microtubules as well as actin filaments, leading to a "hand-over" from microtubules to actin at the cortex (Bi *et al.*, 1997; Rogers and Gelfand, 1998; Rodionov *et al.*, 1998; Brown, 1999).

Our observations demonstrate that microtubules, rather than actin, are essential for delivery and fusion of post-Golgi cargo to the plasma membrane. In pursuit of understanding the mechanism of constitutive exocytosis, several questions remain to be answered: What is the necessary fusion machinery in vivo? Are there interactions between the cytoskeleton and components of the fusion machinery? When and how are the components of this fusion machinery delivered to these fusion sites?

ACKNOWLEDGMENTS

We thank Natalie de Souza and Jyoti Jaiswal for discussions and comments on the manuscript. We thank Mombaerts laboratory for supplying the tau-GFP and Yunbo Chen from E. Rodriguez-Boulan laboratory for supplying the LDLRa18-GFP. J.S. and S.M.S. are supported by NSF BES 0110070 and BES-0119468 (to S.M.S.).

REFERENCES

Axelrod, D. (1989). Total internal reflection fluorescence microscopy. Methods Cell Biol. *30*, 245–270.

Bi, G.Q., Morris, R.L., Liao, G., Alderton, J.M., Scholey, J.M., and Steinhardt, R.A. (1997). Kinesin- and myosin-driven steps of vesicle recruitment for Ca^{2+}-regulated exocytosis. J. Cell Biol. *138*, 999–1008.

Brown, S.S. (1999). Cooperation between microtubule- and actin-based motor proteins. Annu. Rev. Cell Dev. Biol. *15*, 63–80.

Cramer, L.P., and Mitchison, T.J. (1995). Myosin is involved in postmitotic cell spreading. J. Cell Biol. *131*, 179–189.

De Camilli, P., Benfenati, F., Valtorta, F., and Greengard, P. (1990). The synapsins. Annu. Rev. Cell Biol. *6*, 433–460.

Fesce, R., and Meldolesi, J. (1999). Peeping at the vesicle kiss. Nat. Cell Biol. *1*, E3–E4.

Hirschberg, K., Miller, C.M., Ellenberg, J., Presley, J.F., Siggia, E.D., Phair, R.D., and Lippincott-Schwartz, J. (1998). Kinetic analysis of secretory protein traffic and characterization of Golgi to plasma membrane transport intermediates in living cells. J. Cell Biol. *143*, 1485–1503.

Humeau, Y., Doussau, F., Vitiello, F., Greengard, P., Benfenati, F., and Poulain, B. (2001). Synapsin controls both reserve and releasable synaptic vesicle pools during neuronal activity and short-term plasticity in *Aplysia*. J. Neurosci. *21*, 4195–4206.

Huttner, W.B., Schiebler, W., Greengard, P., and De Camilli, P. (1983). Synapsin I (protein I), a nerve terminal-specific phosphoprotein. III. Its association with synaptic vesicles studied in a highly purified synaptic vesicle preparation. J. Cell Biol. *96*, 1374–1388.

Kreitzer, G., Marmorstein, A., Okamoto, P., Vallee, R., and Rodriguez-Boulan, E. (2000). Kinesin and dynamin are required for post-

Golgi transport of a plasma-membrane protein. Nat. Cell Biol. *2*, 125–127.

Lang, T., Wacker, I., Wunderlich, I., Rohrbach, A., Giese, G., Soldati, T., and Almers, W. (2000). Role of actin cortex in the subplasmalemmal transport of secretory granules in PC-12 cells. Biophys. J. *78*, 2863–2877.

Lippincott-Schwartz, J., Roberts, T.H., and Hirschberg, K. (2000). Secretory protein trafficking and organelle dynamics in living cells. Annu. Rev. Cell Dev. Biol. *16*, 557–589.

Llinas, R., Gruner, J.A., Sugimori, M., McGuinness, T.L., and Greengard, P. (1991). Regulation by synapsin I and Ca(2+)-calmodulin-dependent protein kinase II of the transmitter release in squid giant synapse. J. Physiol. *436*, 257–282.

McNew, J.A., Parlati, F., Fukuda, R., Johnston, R.J., Paz, K., Paumet, F., Sollner, T.H., and Rothman, J.E. (2000). Compartmental specificity of cellular membrane fusion encoded in SNARE proteins. Nature *407*, 153–159.

Mitchison, T., and Kirschner, M. (1984). Dynamic instability of microtubule growth. Nature *312*, 237–242.

Morris, C.E., and Homann, U. (2001). Cell surface area regulation and membrane tension. J. Membr. Biol. *179*, 79–102.

Oheim, M., Loerke, D., Stühmer, W., and Chow, R.H. (1998). The last few milliseconds in the life of a secretory granule: docking, dynamics and fusion visualized by total internal reflection fluorescence microscopy (TIRFM). Eur. Biophys. J. Biophys. Lett. *27*, 83–98.

Pfeffer, S.R. (1994). Rab GTPases: master regulators of membrane trafficking. Curr. Opin. Cell Biol. *6*, 522–526.

Polishchuk, R.S., Polishchuk, E.V., Marra, P., Alberti, S., Buccione, R., Luini, A., and Ironov, A.A. (2000). Correlative light-electron microscopy reveals the tubular-saccular ultrastructure of carriers operating between Golgi apparatus and plasma membrane. J. Cell Biol. *148*, 45–58.

Rodionov, V.I., Hope, A.J., Svitkina, T.M., and Borisy, G.G. (1998). Functional coordination of microtubule-based and actin-based motility in melanophores. Curr. Biol. *8*, 165–168.

Rogers, S.L., and Gelfand, V.I. (1998). Myosin cooperates with microtubule motors during organelle transport in melanophores. Curr. Biol. *8*, 161–164.

Rudolf, R., Salm, T., Rustom, A., and Gerdes, H.H. (2001). Dynamics of immature secretory granules: role of cytoskeletal elements during transport, cortical restriction, and F-actin-dependent tethering. Mol. Biol. Cell *12*, 1353–1365.

Rusan, N.M., Fagerstrom, C.J., Yvon, A.M., and Wadsworth, P. (2001). Cell cycle-dependent changes in microtubule dynamics in living cells expressing green fluorescent protein-α tubulin. Mol. Biol. Cell *12*, 971–980.

Ryan, T.A. (1999). Inhibitors of myosin light chain kinase block synaptic vesicle pool mobilization during action potential firing. J. Neurosci. *19*, 1317–1323.

Sammak, P.J., and Borisy, G.G. (1988). Direct observation of microtubule dynamics in living cells. Nature *332*, 724–726.

Saxton, W.M., Stemple, D.L., Leslie, R.J., Salmon, E.D., Zavortink, M., and McIntosh, J.R. (1984). Tubulin dynamics in cultured mammalian cells. J. Cell Biol. *99*, 2175–2186.

Schmoranzer, J., Goulian, M., Axelrod, D., and Simon, S.M. (2000). Imaging constitutive exocytosis with total internal reflection fluorescence microscopy. J. Cell Biol. *149*, 23–32.

Schulze, E., and Kirschner, M. (1986). Microtubule dynamics in interphase cells. J. Cell Biol. *102*, 1020–1031.

Seitz, A., Kojima, H., Mandelkow, E.M., Song, Y.H., and Mandelkow, E. (2002) Single-molecule investigation of the interference between kinesin, tau and MAP2c. EMBO Journal *21*, 4896–4905.

Stephens, D.J., and Pepperkok, R. (2001). Illuminating the secretory pathway: when do we need vesicles? J. Cell Sci. *114*, 1053–1059.

Steyer, J.A., Horstmann, H., and Almers, W. (1997). Transport, docking and exocytosis of single secretory granules in live chromaffin cells. Nature *388*, 474–478.

Toomre, D., Keller, P., White, J., Olivo, J.C., and Simons, K. (1999). Dual-color visualization of trans-Golgi network to plasma membrane traffic along microtubules in living cells. J. Cell Sci. *112*, 21–33.

Toomre, D., Steyer, J.A., Keller, P., Almers, W., and Simons, K. (2000). Fusion of constitutive membrane traffic with the cell surface observed by evanescent wave microscopy. J. Cell Biol. *149*, 33–40.

Trinczek, B., Ebneth, A., Mandelkow, E.M., and Mandelkow, E. (1999). Tau regulates the attachment/detachment but not the speed of motors in microtubule-dependent transport of single vesicles and organelles. J. Cell Sci. *112*, 2355–2367.

Wacker, I., Kaether, C., Kromer, A., Migala, A., Almers, W., and Gerdes, H.H. (1997). Microtubule-dependent transport of secretory vesicles visualized in real time with a GFP-tagged secretory protein. J. Cell Sci. *110*, 1453–1463.

Weber, T., Zemelman, B.V., McNew, J.A., Westermann, B., Gmachl, M., Parlati, F., Sollner, T.H., and Rothman, J.E. (1998). SNAREpins: minimal machinery for membrane fusion. Cell *92*, 759–772.

Zerial, M., and McBride, H. (2001). Rab proteins as membrane organizers. Nat. Rev. Mol. Cell Biol. *2*, 107–117.